PII: S0955-2219(98)00160-5

0955-2219/98/$—see front matter

Semiconductor Properties of Thin and Thick Film Ga_2O_3 Ceramic Layers

Adalbert Feltz[a]* and Ernst Gamsjäger[b]

[a]Siemens Matsushita Components OHG, Siemensstraße 43, A-8530 Deutschlandsberg, Germany
[b]Steinel AG, Allmeindstraße 10, CH-8840 Einsiedeln, Switzerland

(Received 4 April 1998; accepted 16 June 1998)

Abstract

The semiconductor behavior of thin and thick film β Ga_2O_3 layers is studied by measuring the resistivity as a function of oxygen partial pressure and temperature in the range up to 900°C. As for ZnO and SnO_2 a relatively high initial oxygen vacancy defect concentration has to be assumed for β Ga_2O_3. However, the conductivity is by many orders of magnitude lower and the activation energy by about 1 order of magnitude higher. With increasing temperature a change at about 810 ± 50°C from a lower value of the activation energy $E_A(2) = 1{\cdot}6 \pm 0{\cdot}1$ eV to a higher one $E_A(1) = 2{\cdot}4 \pm 0{\cdot}1$ eV is observed at thin film ceramic layers thus leading to the assumption that oxygen cleavage in contact with the atmosphere is achieved in the upper range. Contrary to the band model which is convincingly founded for ZnO and SnO_2 in the literature, polaron hopping seems to be the more suitable model for analysis of the conductivity data of β Ga_2O_3. The lower value $E_A(2)$ is interpreted as the polaron hopping energy at approximately constant charge carrier concentration. On the other hand, in the high temperature range above T_{ch} the charge carrier density is varying. However, at the applied measuring conditions, this variation remains below the initial oxygen vacancy defect concentration. Corresponding to formula I $Ga^{III}_{2-2x}Ga^{II}_{2x}{}'O_{3-x}V^{\cdot\cdot}_{O,x}$ and formula II $Ga^{III}_{2-x}Ga^{I}_{x}{}''O_{3-x}V^{\cdot\cdot}_{O,x}$ two different structures for the oxygen vacancy defects in β Ga_2O_3 are discussed. The measurements seem to confirm formula I. However, provided that there is an equilibrium between states corresponding to formula II and I, the assumption of double occupied Ga^I states is also consistent with the experimental results.

*To whom correspondence should be addressed. Fax: +43 3462 800373; e-mail: adalbertfeltz@siemens.dlb1.de

Zusammenfassung

Das Halbleiterverhalten keramischer Dünn- und Dickschichten von β-Ga_2O_3 wird durch Messung des Widerstandes in Abhängigkeit vom Sauerstoffpartialdruck und der Temperatur im Bereich bis zu 900°C untersucht. Ähnlich wie beim ZnO und SnO_2 ist auch für β-Ga_2O_3 eine relativ hohe Konzentration von Sauerstoffleerstellen in Betracht zu ziehen. Die Leitfähigkeit ist jedoch um Größenordnungen geringer und die Aktivierungsenergie um etwa eine Größenordnung höher. Bei steigender Temperatur wird etwa im Bereich $T_{ch} = 810 \pm 50$°C eine Änderung von einem niedrigeren Wert der Aktivierungsenergie $E_A(2) = 1.6 \pm 0{\cdot}1$ eV zu einem höheren Wert $E_A(1) = 2{\cdot}4 \pm 0{\cdot}1$ eV gefunden, was zu der Schlußfolgerung Anlaß gibt, daß sich im oberen Temperaturbereich das Sauerstoffleerstellen-Bildungsgleichgewicht im Kontakt mit der umgebenden Atmosphäre einstellt. Das Bändermodel zur Beschreibung der Leitfähigkeit von ZnO und SnO_2 ist experimentell in der Literatur gut begründet. Im β-Ga_2O_3 ist dagegen auf Polaronenhopping lokalisierter Ladungen zu schließen. Der niedrigere Wert $E_A(2)$ wird als Polaronenhopping-Energie bei annähernd konstanter Ladungsträgerkonzentration interpretiert. Dagegen variiert die Ladungsträgerkonzentration im Hochtemperaturbereich oberhalb T_{ch}. Unter den angewandten Meßbedingungen bleibt diese Variation jedoch unterhalb der Sauerstoffleerstellenkonzentration, die in der keramischen β-Ga_2O_3-Schicht bereits vom Herstellungsprozeß enthalten ist. Den Formeln I $Ga^{III}_{2-2x}Ga^{II}_{2x}{}'O_{3-x}V^{\cdot\cdot}_{O,x}$ und II $Ga^{III}_{2-x}Ga^{I}_{x}{}''O_{3-x}V^{\cdot\cdot}_{O,x}$ entsprechend werden zwei unterschiedliche Strukturen für die Sauerstoff-Defektzentren in Betracht gezogen. Die Meßergebnisse sprechen für das Vorliegen von Sauerstoffleerstellen gemäß Formel I. Unter der Annahme, daß zwischen den beiden Strukturen im Sinne einer Komproportionierung bzw. Disproportionierung ein Gleichgewicht besteht,

kann jedoch auch Formel II mit den experimentellen Befunden in Einklang gebracht werden.

1 Introduction

The semiconductor behavior of Ga_2O_3 at elevated temperatures has already been studied in earlier papers.[1–4] Fleischer and Meixner[5–11] were the first to make these properties accessible for gas sensing purposes. At sufficiently high temperature equilibrium with oxygen in the surrounding atmosphere results in the formation of oxygen defects and at the same time negatively charged carriers are leaved behind in the lattice giving rise to *n*-type conductivity in dependence on oxygen partial pressure and temperature. β-Ga_2O_3 is thermodynamically in a stable state showing no phase transformation up to high temperature.[12]

An interdigital stucture of Pt electrodes mounted upon an alumina substrate and covered with a Ga_2O_3 thin film layer of 1 to 2 μm thickness by sputtering has been proposed to be a suitable setup for detecting low concentrations of gases, e.g. of hydrogen, hydrocarbons or carbonmonoxide.[13–17] With increasing partial pressure these reducing gases generate an increasing concentration of oxygen vacancy defects in the Ga_2O_3 thin film layer. However, defect formation takes place in competition with the contrary reaction initiated by the presence of oxygen, e.g. of air, which tends to occupy these vacancies. A steady state of the rates of these two opposite reactions may be assumed in the range of about $650°C < T < 900°C$ thus leading to a definite conductivity which at constant oxygen partial pressure and temperature depends only on the type and concentration of the reducing gas.

In the range of 900 to 1000°C equilibrium conditions are valid, which are suitable for oxygen sensing.[18] In this range, effects resulting from small parts of reducing gases are negligible provided that the partial pressure p_{O2} is sufficiently higher than the partial pressure of the reducing impurities. On the other hand, in the lower range of about 600 to 850°C hydrogen, carbonmonoxide, methane or other hydrocarbons and alcohols at concentrations of some ten to thousand ppm are sensitively detectable in air, i.e. even in excess of oxygen. Therefore, a steady state is suggested to be assumed based on the competition of the two reactions mentioned above.

Fleischer and Meixner[19] studied the conductivity and electron mobility in single crystals and polycrystalline ceramic samples of Ga_2O_3. Despite of these studies, as in earlier papers,[1–4] deficiencies persist regarding the consideration of effects which result from oxygen partial pressure variation. Complete analysis of the high temperature semiconductor behavior of Ga_2O_3 layers taking into consideration the equilibrium with oxygen partial pressure seems to be still outstanding. It is the aim of this paper to study the conductivity of thin and thick film ceramic layers of Ga_2O_3 in dependence on temperature and oxygen partial pressure in order to reveal the boundary conditions of equilibrium.

2 Defect Chemistry of Ga_2O_3

By thermodynamic reasons Ga_2O_3 has to be nonstoichiometric at a given oxygen partial pressure and variation of temperature. However, only in the range of sufficiently high temperature the equilibrium concentration of oxygen vacancies V_O will be able to follow the variation of temperature and oxygen partial pressure without relaxation. Oxygen vacancy formation corresponding to

$$Ga_2O_3 \iff Ga_2O_{3-x}V_{O,x} + x/2\,O_2 \quad (1)$$

is coupled with the generation of mobile charge carriers. This is shown by the following more extended formulations indicating two possible stuctures of the oxygen vacancy defects $V_{O,x}$:

formula I $Ga^{III}_{2-2x}Ga^{II}_{2x}{}'O_{3-x}V^{\bullet\bullet}_{O,x}$ and formula II $Ga^{III}_{2-x}Ga^{I}_{x}{}''O_{3-x}V^{\bullet\bullet}_{O,x}$

The $2x$ defect electrons leaved behind by oxygen cleavage are localized forming $2x$ Ga^{II} which are coupled with x oxygen vacancies by Coulomb attraction yielding x defect complexes $[Ga^{II}_2{}'/V^{\bullet\bullet}_O]$ (formula I). The latter appears to be uncharged at larger distances, i.e. a thermal activation energy has to be expected for negative charge carrier escape from such a defect state. Moreover, because of the close distance in the defect triplet the $2x$ Ga^{II} states could give rise to a covalent-like interaction forming x weak Ga–Ga bonds which also suggest the occurrence of a thermal activation in charge carrier transport. Ga–Ga bonds are known for compounds with Ga in the lower valency state, e.g. in the layer-like crystal structure of GaS and GaSe.[20]

On the other hand, the more polar compound $GaCl_2$ has a salt-like type structure $[Ga^I]^+[Ga^{III}Cl_4]^-$.[21] The nature of the chemical bond in Ga_2O_3 seems to be also more polar as for the chalcogenides. Of course, in consistence with the heavier homologoues of Ga in the periodic table Ga^I formation has to be also considered as a possibility of defect formation, i.e. pairwise electron occupation could be preferred in the result of Ga^{II} disproportionation leading to a defect pair

$[Ga^{I''}V_O^{\bullet\bullet}]$ (formula II). Commonly, because of interelectronic repulsion pairing should be less favored or, in other words, the electron correlation energy U_{LP} of Lone Pair formation is positive. Anderson[22] pointed out, that by reason of the polarizability of the environment in the lattice the effective electron correlation energy $U_{eff} = U_{LP} - \beta^2/2\alpha$ can become negative. β is a measure of the polarizability, α describes the force constant of elastic stress caused by polarization in the localized polaron state of a charge carrier. In such a disproportionation state the first ionization energy has to be higher than the second one and therefore always pairwise thermal excitation will take place in charge carrier transport.

Actually, of all structural and electronic defects the one that requires the smallest free energy of formation will be present at the highest concentration. All of the possible defect states caused by oxygen cleavage can be interpreted as polaron states suggesting the occurrence of thermal activation in polaron hopping charge carrier transport.

The following equation will be obtained assuming diffusion like jumping of polarons, i.e. hopping of localized charge carriers excited by a phonon frequency ν_0 takes place. The mobility μ may be expressed by the Nernst Einstein equation $\mu = (e/kT)\ D$ with $D = a^2(1-w)\nu = a^2(1-w)\nu_0\ \exp[-E_\sigma/kT]$. $(1-w)$ describes the probability to meet unoccupied Ga^{III} sites in the neighborhood of a Ga^{II} or Ga^{I} polaron state:

$$\sigma = ne\mu = ne\frac{ea^2(1-w)}{kT}v_0 e^{-\frac{E_\sigma}{kT}} = ne\mu_0^{-\frac{E_\sigma}{kT}} \qquad (2)$$

If n is replaced by the expression $n = N_1 w/V$ with N_1 as the total number of Ga-sites in the sample volume V and w is interpreted as the probability of their occupation by an electron (Ga^{II}) and if the ratio $N_1/V = n_0/a^3$ is used with n_0 as the number of Ga atoms in the jump volume a^3, eqn (2) then leads to

$$\sigma = \frac{n_0 v_0 e^2 w(1-w)}{akT} e^{-\frac{E_\sigma}{kT}} \qquad (3)$$

Corresponding to formula I or II, w may be expressed by the mole fraction $x_{Ga^{II}} = w = n_{Ga^{II}}/(n_{Ga^{II}}$ or $n_{Ga^{III}}\ x_{Ga^{I}} = w = n_{Ga^{I}}/(n_{Ga^{I}}\ n_{Ga^{III}})$, respectively, and assuming for $n_{Ga^{II}}$ or $n_{Ga^{I}} << n_{Ga^{III}}$, the equation

$$\sigma = \frac{n_0 v_0 e^2}{akT} x_{Ga^{II(I)}} e^{-\frac{E_\sigma}{kT}} \qquad (4)$$

is obtained. The relation to oxygen partial pressure is introduced by the law of mass action applied to the defect formation equilibrium (1). Corresponding to formula I the relation

$$K_p = p_{O_2}^{1/2} x_{v_o} x_{Ga^{II}}{}^2 \qquad (5)$$

has to be expected, which together with $x_{v_o-} = (1/2)x_{Ga}{}^{II}$ leads to

$$x_{Ga^{II}} = (2K_p)^{1/3} p_{o_2}^{-1/6} \qquad (6)$$

i.e. at constant temperature the conductivity should be a function of oxygen partial pressure with a slope of $-1/6$ in the Kröger–Vink diagram.[23]

On the other hand, in the range of lower temperature the initial concentration of donors in the lattice, consisting possibly predominantly of oxygen vacancies, could be very much higher than the contribution generated by oxygen partial pressure variation. Thus starting from lower temperature, a constant value $x_{VO} = C_1$ should be valid yielding a slope of $-1/4$

$$x_{Ga^{II}} = (K_p/C_1)^{1/2} p_{o_2}^{-1/4} \qquad (7)$$

Such a relation has been often observed for oxides up to relatively high temperatures. An analogous relation results from formula II for the defect equilibrium

$$K_p = p_{O_2}^{1/2} x_{v_o} x_{Ga^{I}} \qquad (8)$$

yielding

$$x_{Ga^{I}} = (K_p)^{1/2} p_{o_2}^{-1/4} \qquad (9)$$

Hence, if again $x_{VO} = C_1'$ is assumed to be constant in the low temperature range, the relation

$$x_{Ga^{I}} = \frac{K_p}{C_1'} p_{o_2}^{-1/2} \qquad (10)$$

is expected to be observed in the experimental results

Temperature dependence in the most simple approximation requires to consider $\Delta G^0(T) = \Delta H^0 - T\Delta S^0$ together with $Kp = \exp[-\Delta\ G^0(T)/RT]$. Application to eqn (4) in combination with (7) leads to

$$\sigma = \frac{n_0 v_0 e^2}{ak}\frac{1}{T}\frac{1}{\sqrt{C_1}} e^{\frac{\Delta S^0}{2R}} p_{O_2}{}^{-1/4} e^{-\frac{\Delta H^0 + 2E_\sigma}{2RT}} \qquad (11)$$

or together with $\frac{n_0 v_0 e^2}{ak} = C_2$, $e^{\frac{\Delta S^0}{2R}} = C_3$ and $\sigma = \frac{1}{R}\frac{L}{A} = \frac{1}{R}\frac{1}{C_4}$, the relation

$$\frac{T}{R} = \frac{C_2 C_3 C_4}{\sqrt{C_1}} p_{o_2}^{-1/4} e^{-\frac{\Delta H^0 + 2E_\sigma}{2RT}} \qquad (12)$$

is obtained for a given sample. In the range where the constant value $x_{VO} = C_1$ would be valid, the thermal activation energy of polaron hopping should be expressed by

$$E_A = \frac{\Delta H^0 + 2E_\sigma}{2} \tag{13}$$

On the other hand, at higher temperature where $x_{VO} > C_1$ could occur, eqn (4) should be combined with eqn (6) which leads to

$$\frac{T}{R} = 2^{1/3} C_2 C_3' C_4 p_{o_2}^{-1/6} e^{-\frac{\Delta H_0 + 3E_\sigma}{3RT}} \tag{14}$$

with $e^{\frac{\Delta s^0}{3R}} = C_3'$ and

$$E_A = \frac{\Delta H^0 + 3E_\sigma}{3} \tag{15}$$

for the activation energy.

Furthermore, if defect formation according to formula (II) should be favoured, eqns (4) and (8) provide the relation

$$\frac{T}{R} = C_2 C_3 C_4 p_{o_2}^{-1/4} e^{-\frac{\Delta H^0 + 2E_\sigma}{2RT}} \tag{16}$$

Finally, if the initial excess concentration x_{Ga}^I would be higher than the contribution caused by oxygen partial pressure variation, a constant value $x_{Ga}^I = C_1'$ has to be taken into account, which together with $e^{\Delta s^0/R} = C_3''$ leads to the relation

$$\frac{T}{R} = \frac{C_2 C_3'' C_4}{\sqrt{C_1'}} p_{o_2}^{-1/2} e^{-\frac{\Delta H^0 + E_\sigma}{RT}} \tag{17}$$

3 Experimental

Sample preparation has been carried out by starting from 2×2 inch alumina substrates of 0·63 mm thickness. After pre-treatment of the surface of the substrate a Pt thin film layer of about 2 μm thickness was deposited on the one side by sputtering. Photolithographic processing leads to a pattern of several hundred single elements consisting of interdigital stages of 20 μm width with distances of about 20 μm. The back side was also equipped by photolithography with a pattern of heating meanders of Pt.[14] The semiconducting Ga_2O_3 layer between and above the interdigital electrodes on the front side has been prepared in a thin film version by sputtering (1 or 2 μm) and in a thick film version by screen printing (about 10 μm). Annealing at about 850°C (10 h) transforms the sputtered amorphous thin film into polycrystalline β Ga_2O_3. Adherence of the screen printed thick film layers requires application of a sintering temperature of about 1000°C. Finally, cutting provides the single sensor samples. For electrical measurements they were completed by bonding of Pt wires of 100 μm thickness at the contact pads of the Pt heater on the back and also at the pads of the Pt interdigital structure of the Ga_2O_3 sensor on the front side.

For measuring the resistivity as a function of temperature at constant oxygen partial pressure, the small sensor elements were brought into a gas stream of definite composition, e.g. of air or wet or dry nitrogen with a defined oxygen partial pressure. Isothermic measurements were carried out changing the oxygen partial pressure in the gas stream. In order to adjust a definite temperature at the sensor sample electrical heating of the Pt thin film meander structure has been performed. The applied voltage was controlled by the Pt resistivity temperature characteristic using a suitable electronic processor. For calibration a thermo camera was used.

Measurements of the resistivity R of the Ga_2O_3 layers as a function of oxygen partial pressure p_{O2} started after adjustment of a defined temperature T. The applied voltage was limited to about 0·5 V using a voltage drop circuit in order to avoid polarization effects at the contacts of the sample. Even at high temperature the Ga_2O_3 layer is still a comparatively high resistive material.

Measurements at constant oxygen partial pressure as a function of temperature revealed that the electrical data depend sensitively on thermal pretreatment of the samples. Fast cooling from high temperature immediately after annealing for crystallization of the sputtered Ga_2O_3 layer leads to lower resistivity values indicating a higher concentration of defects with excitable carriers. On the other hand, adsorption of oxygen or humidity at the surface during seating of the samples in common atmosphere give rise to trapping of charge carriers, which leads to an opposite effect.

The temperature was changed by about 15 K in the $R(T)$ measurements waiting at every step several minutes for thermal equilibration. The samples were submitted to three different kinds of thermal treatment in close relation with up↑ and down↓ measurements of the $R(T)$ curves. Commonly, repeating of the measurements revealed relaxation as a consequence of slow thermal cycling.

A. First measurement (1) up↑ and (1) down↓ between 550 and 1000°C, 11 days seating at room temperature in air, second measurement (2) up↑ and (2) down↓.

B. First measurement (1) up↑ and (1) down↓ between 550 and 1000°C, 14 h keeping at 1000°C by electrical heating of the Pt meander structure, fast cooling and after that immediately second measurement (2) up↑ and (2) down↓.

C. 14 h keeping at 1000°C by heating the Pt meander structure, fast cooling and first measurement (1) up↑ and (1) down↓ between 550 and 1000°C, and after that immediately second measurement (2) up↑ and (2) down↓.

4 Experimental results

The results are expected to infer to the defect type and also to a rough estimation of their concentration in the material. Corresponding to formula I or II, eqns (12) or (17) should be valid for changing the oxygen partial pressure at a constant lower temperature yielding in the double logarithmic plot a slope of $-1/4$, or $-1/2$, respectively. On the other hand, at a constant higher temperature a relation corresponding to eqns (14) or (16) with a slope of $-1/6$ or $-1/4$ is expected to be observed. Hence, a change of the slope of the conductivity as a function of oxygen partial pressure should indicate a transition from a constant value of $x_{V_O^{\bullet\bullet}}$ to a variable one. On the other hand, following eqns (12), (14) or (17), measurements of the conductivity as a function of temperature are suggested to reveal a change in the activation energy indicating the onset temperature of equilibrium for oxygen vacancy defect formation.

4.1 Semiconducting properties of sputtered β-Ga_2O_3 thin films

Figure 1 shows the experimental data in terms of (T/R) as a function of oxygen partial pressure p_{O2} for three groups of sensors measured at 700, 750 and 830°C. The double logarithmic plot elucidates straight correlation of the measuring points yielding a slope near $-1/4$ without any break. The isothermic measurements were carried out between 600 and 900°C and always the same slope of $-1/4$ was found. Such a result is consistent with published data.[3,4] Hence, formula I for the defects seems to be supported by these findings because there is no indication for a shift of the slope to $-1/2$ in the range of lower temperature. The latter has to be expected if formula II would be valid. Lowering of the slope from $-1/4$ to $-1/6$ at higher temperature is also missing. Obviously, the oxygen vacancy concentration remains effectively unchanged, i.e. $x_{VO} = C_1$ seems to be valid in the whole range of temperature. Obviously, at this stage eqn (12) in combination with formula I is suggested to supply the most probable model for the state of defects in polycrystalline β Ga_2O_3 thin film layers. Analysis of the pre-exponential factor in Fig. 1 fails because of uncontrolled variations of the geometry at the contacts of the sensor specimens.

Figure 2 shows an Arrhenius plot of the values (T/R) measured as a function of temperature for a typical sample with a thermal treatment corresponding to A. The values below 650°C are artificial because of retardation in achieving equilibrium. Moreover, the first heating up curve 1(↑) shows a significant deviation to lower conductivity values, which has been always observed after seating the specimens in air. Presumably, adsorption of humidity or impurities from the atmosphere are responsible for charge carrier

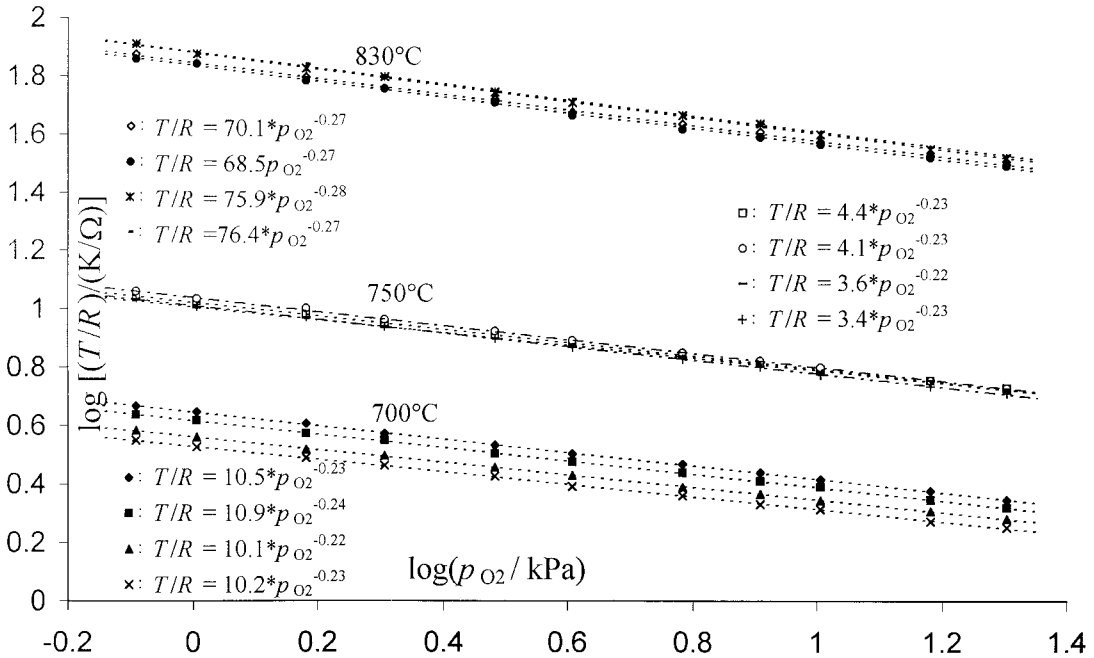

Fig. 1. Double logarithmic plot of the data (T/R) measured as a function of oxygen partial pressure at 700, 750 and 830°C of three groups of β Ga_2O_3 thin film layer samples.

trapping. Therefore, the first run was excluded from analysis for samples of type A and B. On the other hand, the curves 1(↓), 2(↑) and 2(↓) of Fig. 2 show satisfactory accordance. The occurrence of a change of the slope at the temperature T_{ch} has to be noticed indicating a transition from a lower value of the activation energy $E_A(2)$ to a higher value $E_A(1)$. The data are summarized in Table 1.

Analysis of all of the measuring runs of the two specimens A and of B1(↓) provide an average value $T_{ch} = 775 \pm 14°C$ and for $E_A(1) = 2{\cdot}45 \pm 0{\cdot}05$ eV and $E_A(2) = 1{\cdot}9 \pm 0{\cdot}2$ eV. The latter value is interpreted as the activation energy E_σ of polaron hopping assuming that ΔH^0 in eqn (12) is near to zero below T_{ch}, i.e. as long as the defect formation equilibrium is effectively frozen in. Therefore, the charge carrier concentration is assumed to be approximately independent of temperature in this lower range of temperature, i.e. the activation energy is predominantly assigned to the mobility of polarons.

On the other hand, at higher temperature above T_{ch} equilibrium is achieved within measuring time, thus leading to an additional term ΔH^0 in the activation energy. Changing of the charge carrier density has now to be taken into consideration. As a consequence, the enthalpie of oxygen defect formation in β Ga_2O_3 is inferred to be accessible from electrical measurements. However, even at a temperature of about 900°C still the initial donor concentration seems to prevail. Based on eqn (13) the values $E_A(2) = 1{\cdot}9 \pm 0{\cdot}2$ eV and $E_A(1) = 2{\cdot}45 \pm 0{\cdot}05$ eV provide for $\Delta H^0 = 1{\cdot}1 \pm 0{\cdot}5$ eV or 105 ± 50 kJ mole.

Figure 3 shows the results of a typical sample with thermal treatment B. Again interpretation of run 1(↑) is omitted. Fourteen h keeping at 1000°C and fast cooling after the first measuring cycle is followed by the second 2(↓) and third run 2(↑). Obviously, the increased conductivity in the low temperature range, i.e. below T_{ch}, is the result of the higher density of oxygen vacancies which are formed during annealing at 1000°C and become frozen in at fast cooling. The lower values of the activation energy suggest more shallow defects in the sample, possibly oxygen defects which are nearer to the surface. At the same time, in accordance with expectation the temperature indicating the change of the activation energy is shifted to the higher value $T_{ch} = 850 \pm 30°C$. During measuring of curve 2(↑) the non-equilibrium states become partially relaxed yielding a curve of higher resistivity values in the following run 2(↓). Hence, because of partial equilibration the low temperature slope is increased from $E_A(2) = 1{\cdot}3$ eV for 2(↑) to $E_A(2) = 1{\cdot}5$ eV for 2(↓). On the other hand, in the high temperature range above T_{ch} the value of $E_A(1) = 2{\cdot}3$ eV is again near to the value which was already found for the specimens of type A.

As can be seen from Fig. 4, a similar result is found in the high temperature range for samples with thermal history C (Table 1). In correspondence to the run B2(↑), the first curve C1(↑) measured immediately after 14 h annealing at 1000°C and followed by fast cooling yields in the low temperature range again lower resistivity values and the activation energy is again significantly lower

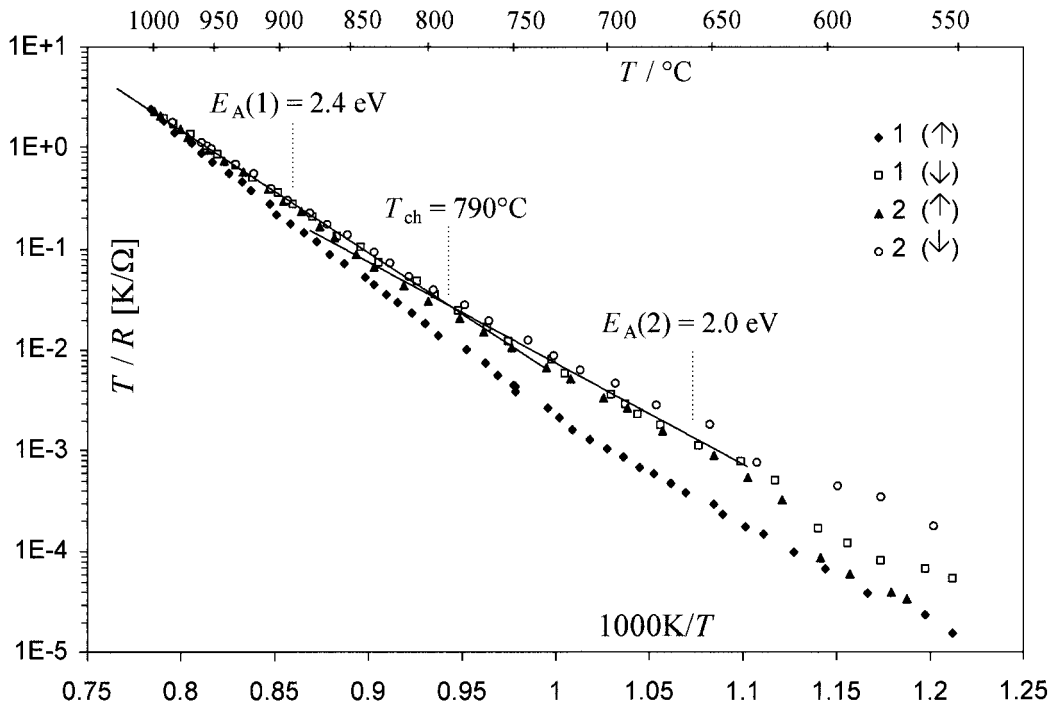

Fig. 2. Arrhenius plot of the date (T/R) as a function of temperature obtained in the runs of up (↑) and down (↓) measurement of the sputtered β Ga_2O_3 thin film specimen 1A according to Table 1.

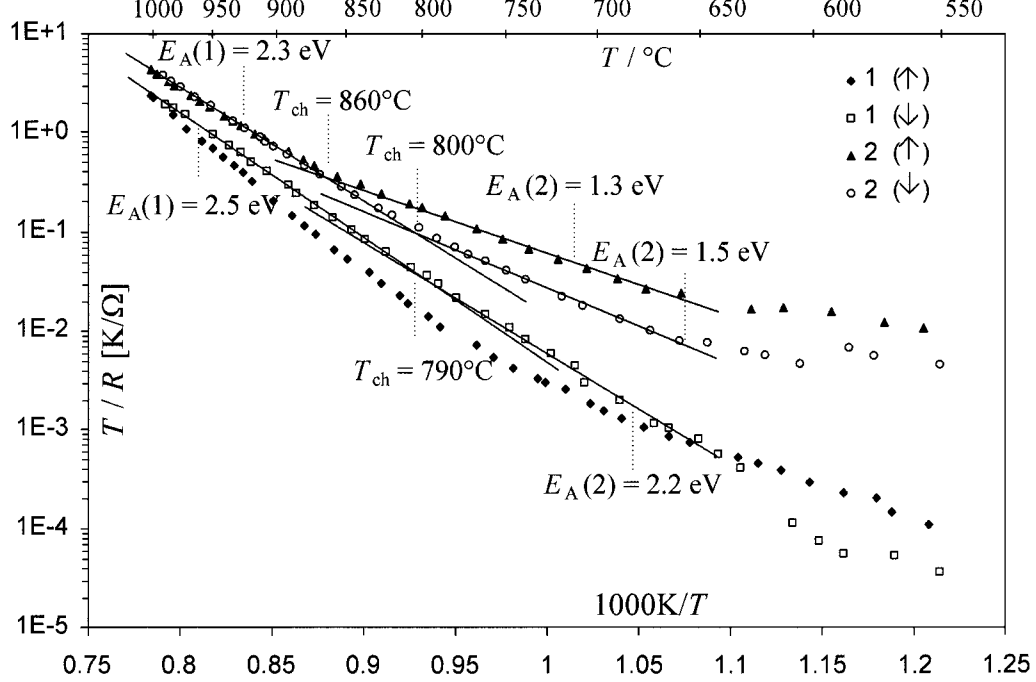

Fig. 3. Arrhenius plot of the date (T/R) as a function of temperature obtained in the runs of up (↑) and down (↓) measurement of the sputtered β Ga_2O_3 thin film specimen 3B according to Table 1.

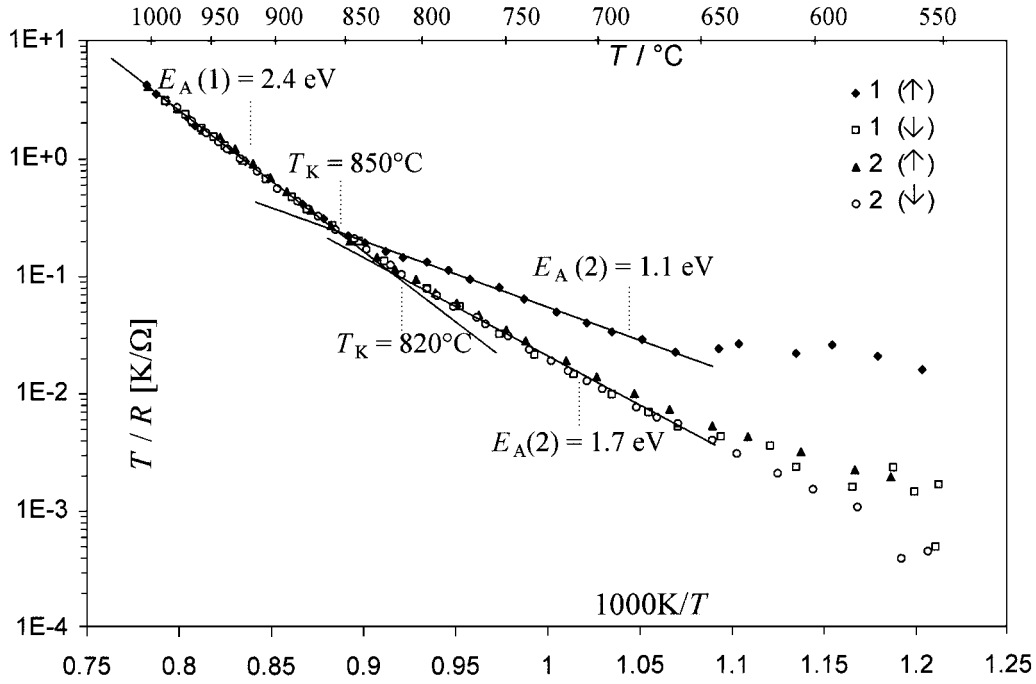

Fig. 4. Arrhenius plot of the date (T/R) as a function of temperature obtained in the runs of up (↑) and down (↓) measurement of the sputtered β Ga_2O_3 thin film specimen 7C according to Table 1.

than in the following runs C1(↓), C2(↑) and C2(↓). The four samples B2(↑) and C1(↑) yield for $E_A(2) = 1{\cdot}33 \pm 0{\cdot}06$ eV, $E_A(1) = 2{\cdot}37 \pm 0{\cdot}06$ eV and $\Delta H^0 = 2{\cdot}1 \pm 0{\cdot}3$ eV. Of course, in the result of annealing at 1000°C the oxygen vacancy concentration is increased. Therefore, the enthalpie of oxygen cleavage corresponding to reaction (1) is expected to tend to higher values the more the higher the concentration of oxygen vacancies in the lattice is.

Finally, the data of samples in the partially relaxed state, i.e. measured in the second and further runs of the type C samples have to be considered. Averaging of the values of the 10 runs B2(↓), C1(↓), C2(↑) and C2(↓) of Table 1 yield $T_{ch} = 830 \pm 16$°C, $E_A(2) = 1{\cdot}7 \pm 0{\cdot}1$ eV, $E_A(1) = 2{\cdot}4 \pm 0{\cdot}1$eV and $\Delta H^0 = 1{\cdot}4 \pm 0{\cdot}4$ eV. Fleischer and Meixner found for polycrystalline β Ga_2O_3 thin film ceramic layers in the high temperature range a value of 2·1 eV.[19]

Table 1. Activation energies $E_A(2)$ and $E_A(1)$ according to the break in the slope of sputtered β-Ga_2O_3 thin film layer samples with different kinds A, B and C of thermal treatment

Sensor sample	*Thermal treatment*	*Measuring curves*	*Temperature* T_{ch}/°C *change of the slope*	$E_A(2)$ *eV*	$E_A(1)$ *eV*
1	A	1(↓),2(↑),2(↓)	790	2·0	2·4
2	A	1(↓),2(↑),2(↓)	760	1.8	2.5
3	B	1(↓)	790	2·2	2·5
		2(↑)	860	1·3	2·3
		2(↓)	800	1·5	2·3
4	B	1(↓)	770	1·8	2·4
		2(↑)	870	1·3	2·4
5	C	1(↑)	890	1·4	2·4
		1(↓)	860	1·6	2·3
		2(↑),2(↓)	830	1·7	2·3
6	C	1(↓),2(↑),2(↓)	840	1·8	2·4
7	C	1(↑)	850	1·1	2·4
		1(↓),2(↑),2(↓)	820	1·7	2·4

4.2 Semiconducting properties of screen printed β-Ga_2O_3 thick films

Figure 5 shows the results of isothermic measurements at 750°C for sreen printed β Ga_2O_3 layers with a thickness of about 10 μm. Again the slope of about $-1/4$ is found for all of the four different sensor samples. Several measurements have been carried out between 700 and 900°C for completion. Always approximately the same value of the slope has been observed.

Figure 6 shows the conduction in terms of (T/R) as a function of temperature at the oxygen partial pressure of air for a thick film sample measured immediately after sintering at 1000°C and fast cooling. Again 10 h annealing at 1000°C has been applied after the first (↑) and second (↓) run. No change in the activation energy is detectable and relaxation is missing as well. The activation energy $E_A(1) = 2{\cdot}23$ eV is near to the high temperature value of the thin film layers. However, the conductivity is by about one order of magnitude lower. Obviously, because of the porous structure of the thick film ceramic layer current paths are restricted to the small contact areas between the grains. On the other hand, there is more surface area available for interaction with oxygen of the atmosphere in the porous thick film sample.

Possibly, by this reason kinetics of equilibrium adjustment corresponding to eqn (1) is shifted to lower temperature. Thin films prepared by sputtering followed by recrystallization from the amorphous state are assumed to have a higher compactness and therefore the bulk could be more inhibited in taking part at the equilibrium, which

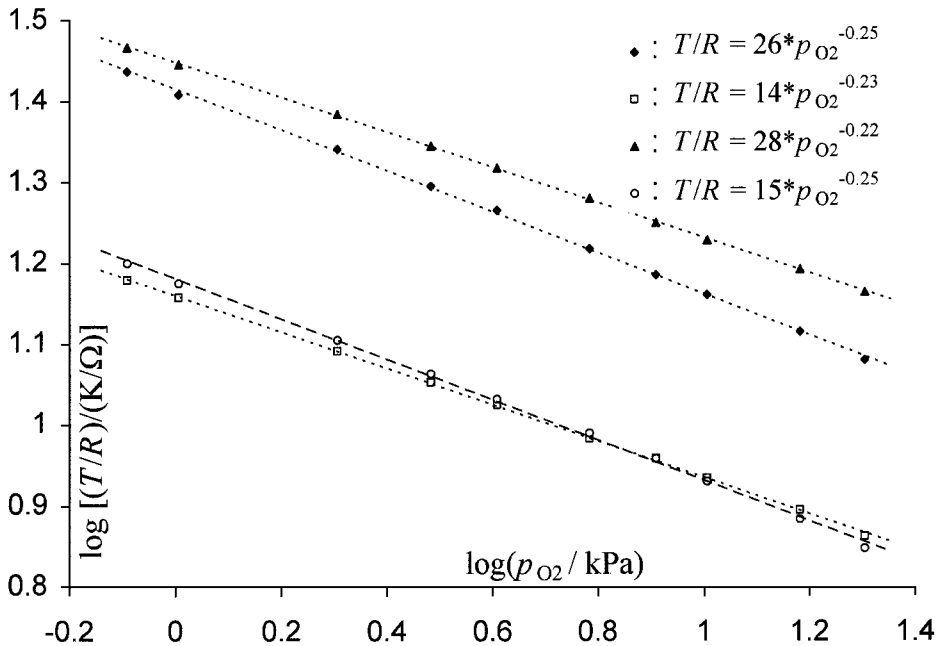

Fig. 5. Double logarithmic plot of the measured data (T/R) of four different screen printed β Ga_2O_3 thick film layer samples as a function of oxygen partial pressure at 750°C.

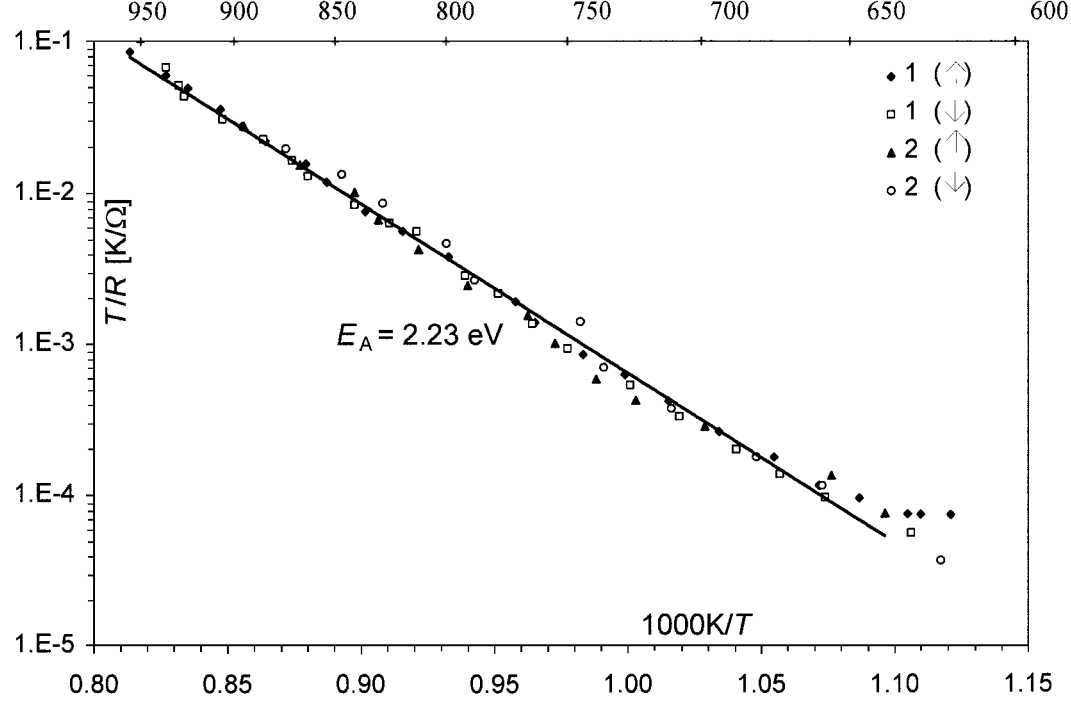

Fig. 6. Arrhenius plot of the date (T/R) as a function of temperature obtained in the runs of up (↑) and down (↓) measurement of a screen printed β Ga_2O_3 thick film specimen.

infers the observed higher value of T_{ch}. As the consequence, polaron hopping at approximately unchanged defect concentration is just still observable in the low temperature range. On the other hand, in the thick porous ceramic films improved kinetics for achieving equilibrium could be responsible for covering this effect.

5 Discussion and conclusions

The enthalpie of oxygen vacancy formation in β Ga_2O_3 of about 1 to 2 eV per mole seems to be in a plausible range. The enthalpie of formation of β Ga_2O_3 at standard conditions is reported to be $-5{,}6$ eV/mole $GaO_{1.5}$.[24] However, in comparison with the neighboured oxides ZnO and SnO_2, the activation energy of about 1·5 eV for β Ga_2O_3, which is found in the low tremperature range below T_{ch} appears to be relatively high. Oxygen cleavage from stoechiometric ZnO generates single occupied defects according to $Zn_{1-2x}Zn'_{2x}O_{1-x}V_O^{\bullet\bullet}$. Their energy level is only about 0·05 eV below the conduction band thus leading in the bulk to the well known high conductivity of ZnO.[25] The electron mobility at room temperature was found to be in the range of 180 cm^2/Vs. SnO_2 has also been shown to be a high mobility semiconductor with negative charge carriers caused by oxygen non-stoechiometry. Corresponding to the formula $Sn^{IV}_{1-2x}Sn^{III}_{2x}{}'O_{1-2x}V_O^{\bullet\bullet}$ single occupied defects have been detected, whose energy is even only about 0·03 eV below the conduction band.[26] Measurements of the conductivity as a function of oxygen partial pressure provide a slope of $-1/4$ for $T <$ 780°C and of $-1/6$ for $T >$ 780°C.[27] Hall effect measurements revealed a mobility of about 240 cm^2/ Vs at room temperature and 50 cm^2/Vs at 730°C,[28] which clearly indicates the suitability of a band model for interpretation. On the contrary to that, β Ga_2O_3 is characterized by a Hall mobility of only about 5 cm^2/Vs at 800°C indicating a positive value of the coefficient of temperature.[19] Therefore, together with the significantly increased activation energy polaron hopping is suggested to be the more appropriate model for interpreting the charge carrier transport of β Ga_2O_3.

Comparing the models presented in this paper, the defect states corresponding to formula I are supported by the experimental results. Sn^{IV} doping of β Ga_2O_3 seems to confirm also these conclusions.[29] The complicated band structure resulting from the structure of β Ga_2O_3 which consists of a network of interconnected tetrahedra and octahedra according to the formula $GaO_{2/2}O_{2/4}GaO_{6/4}$,[12] could also give rise to deeper localization of electrons at the Ga^{II} states. On the other hand, just the different coordination of the two Ga^{III} atoms in the lattice could give rise to a negative electron correlation energy. Hence, Ga^{I} polaron state formation by double occupation could be preferred, e.g. in the sixfold positions of the Ga ions in the structure. The distorted octahedra $Ga^{III}O_{6/4}$ could change to $|Ga^{I}O_{3/4}$ units with a lone pair having only a low

value of negative charge in excess. Such a configuration is well known in the coordination chemistry of compounds of In^{I}, Tl^{I}, Sn^{II} and Pb^{II}.

The problem is to explain that the slope of $-1/4$ is also observed in the lower range of temperature (Figs 1, 2 and 6). However, if one would assume a temperature dependent eqilibrium between the two kinds of electron distribution described by formula I and II, corresponding to $Ga^{I} + Ga^{III} \Longleftrightarrow 2\ Ga^{II}$ comproportionation happens with

$$x_{Ga^{I}} = \frac{x^2_{Ga^{II}}}{K x_{Ga^{III}}} = \frac{x^2_{Ga^{II}}}{C_5} \tag{18}$$

As a consequence, instead of eqn (17) the following relation (19) would become available for analysis: A slope of $-1/4$ in the low temperature range has now to be expected for Ga^{I} defect states in β Ga_2O_3, too.

$$\frac{T}{R} = \frac{C_2 C_3 C_4 \sqrt{C_5}}{\sqrt{C_1'}} p_{o_2}^{-1/4} e^{-\frac{\Delta H^0 + 2E_a}{2RT}} \tag{19}$$

Obviously, similar as for ZnO and SnO_2, the compound β Ga_2O_3 is also in a *n*-conducting state caused by partial oxygen cleavage, which leads to a high initial level of oxygen vacancies.

Acknowledgements

The authors wish to thank Dipl.-Ing Dr Kreitschitz for installation of the measuring equipment and Dipl.-Ing Karner for the careful preparation of the sputtered thin film β Ga_2O_3 samples.

References

1. Lorenz, M. R., Woods, J. F. and Gambino, R. J., Some electrical properties of the semiconductor β Ga_2O_3. *J. Phys. Chem. Solids*, 1976, **28**, 403.
2. Harwig, T., Wubs, G. J. and Dirksen, G. J., Electrical properties of β Ga_2O_3 single crystals. *Solid State Commun.*, 1976, **18**, 1223.
3. Cojocaru, L. N. and Alecu, I. D., Electrical properties of β Ga_2O_3. *Z. Phys. Chem.*, 1973, **84**, 325.
4. Sasaki, T. and Hijikata, K., Electronic conductivity of β Ga_2O_3. *Proc. Inst. Nat. Sci. Nihon Univ., Tokyo*, 1974, **9**, 29.
5. Fleischer, M. and Meixner, H., Sensor zur Erfassung reduzierender Gase. Europ. Patent 90 11 27 81.1, 1990.
6. Fleischer, M. and Meixner, H., Oxygen sensing with long-term stable Ga_2O_3 thin films. Proc. 3rd Int. Meet. Chemical Sensors, Cleveland, OH, 1990, p. 201.
7. Fleischer, M. and Meixner, H., Gallium oxide thin films: a new material for high-temperature oxygen sensors. *Sensors and Actuators B*, 1991, **4**, 437.
8. Fleischer, M., Hanrieder, W. and Meixner, H., Stability of semiconducting gallium oxide thin films. *Thin Solid Films*, 1990, **190**, 93.
9. Fleischer, M., Giber, J. and Meixner, H., H_2-induced changes in electrical conductance of β Ga_2O_3 thin-film systems. *Appl. Phys*, 1992, **A54**, 560.
10. Fleischer, M., Höllbauer, L. and Meixner, H., Effect of the sensor structure on the stability of Ga_2O_3 for reducing gases. *Sensors and Actuators*, 1994, **B18–19**, 119.
11. Fleischer, M. and Meixner, H., Characterization of gas-sensitive, polycrystalline Ga_2O_3 thin films. *J. Mater. Sci. Lett*, 1992, **11**, 1728.
12. Geller, S., Crystal structure of β Ga_2O_3. *J. Chem Phys*, 1960, **33**, 676.
13. Fleischer, M. and Meixner, H., Sensing reducing gases at high temperature using long-term stable Ga_2O_3 thin films. *Sensors and Actuators*, 1992, **B6**, 277.
14. Fleischer, M. and Meixner, H., Improvements in Ga_2O_3 sensors for reducing gases. *Sensors and Actuators*, 1993, **B13–14**, 259.
15. Lampe, U., Fleischer, M. and Meixner, H., Lambda measurement with Ga_2O_3. *Sensors and Actuators*, 1994, **B17**, 187.
16. Fleischer, M. and Meixner, H., A selective CH_4-sensor using semiconducting Ga_2O_3 thin films based on temperature switching of multigas reactions. Proc. 5th Int. Meeting Chemical Sensors, Rome 1994. *Sensors and Actuators*, 1995, **B25**, 544.
17. Fleischer, M., Reti, F., Meixner, H. and Giber, J., Effect of coadsorption of reducing gases on the conductivity of β Ga_2O_3 thin films in the presence of O_2 and CO_2. *Sensors and Actuators*, 1994, **B18–19**, 573.
18. Fleischer, M. and Meixner, H., Oxygen sensing with long-term stable Ga_2O_3 thin films. *Sensors and Actuators*, 1992, **B8**, 115.
19. Fleischer, M. and Meixner, H., Electron mobility in single and polycrystalline Ga_2O_3. *J. Appl. Phys*, 1993, **74**, 300.
20. Hahn, H. and Frank, G., Über die Kristallstruktur des GaS. *Z. anorg. allg. Chem.*, 1955, **278**, 340.
21. Garton, D. and Powell, H. M., The crystal structure of Gallium Dichloride. *J. Inorg. Nucl. Chem.*, 1957, **4**, 84.
22. Anderson, P. W., Model for the Electronic structure of amorphous semiconductors. *Phys. Rev. Lett.*, 1975, **34**, 953.
23. Kröger, F. A., and Vink, H. J., In Relations between the concen-trations of imperfections in crystalline solids, ed. F. Seitz and D. Turnbull. Solid State Physics, Vol. 3. Academic Press, New York, 1956, pp. 307–435
24. Lide, D. R., (ed.), *Handbook of Chemistry and Physics*, 79th edn. 1988–1999, 5–16, CRC Press, Boca Raton, London, New York, Washington, D.C.
25. Kröger, F. A., *The Chemistry of Imperfect Crystals*. North Holland Publishing Company, Amsterdam, 1964.
26. Samson, S. and Fonstadt, C. G., Defect structure and electronic donor levels in stannic oxide crystals. *J. Appl. Phys.*, 1973, **44**, 4618.
27. Maier, J. and Göpel, W., Investigations of the bulk defect chemistry of polycrystalline Tin(IV) oxide. *J. Solid State Chem.*, 1988, **72**, 293.
28. Fonstadt, C. G. and Rediker, R. H., Electrical properties of high-quality stannic oxide crystals. *J. Appl. Phys.*, 1971, **42**, 2911.
29. Frank, J., Fleischer, M., Meixner, H. and Feltz, A., Enhancement of sensitivity and conductivity of semiconducting Ga_2O_3 sensors by doping with SnO_2. Proc. Transducers 97, Chicago, 1997, p. 955.